

Use of Bio-Inspired Keratin Material in Crashworthiness Improvement Using ANSYS Software for Vehicle Frontal Impact Simulation

Aws Namoor^{*}, Majdi Zalloum, Hussein Amro

Department of Mechanical Engineering, Palestine Polytechnic University, Hebron, Palestine

Received 28 Nov 2024

Accepted 12 Mar 2025

Abstract

This paper presents a vehicle-to-vehicle impact analysis using ANSYS Explicit Dynamics simulation software, specifically focusing on a frontal offset impact between two vehicles. The main objective to analyze vehicle crash behavior is to identify potential crashworthiness improvements by use of bio-inspired keratin material. The simulation involves two bumper models. one constructed with bio-inspired keratinized material from horn sheep and the other with a structural steel bumper. The study compares simulation results between the two different material models across a wide collision speed range, utilizing a 3D CAD model of the Audi R8 space frame as the vehicle model. The results indicate that the equivalent von-Mises stress and equivalent plastic strain of the keratin bumper model are higher than those of the structural steel bumper model at low impact speeds. This implies that the keratin bumper model experiences more deformation and energy dissipation at low collision speeds, suggesting that it is safer and possesses higher crashworthiness and energy dissipation compared to the structural steel bumper model.

© 2025 Jordan Journal of Mechanical and Industrial Engineering. All rights reserved

Keywords: frontal impact, crashworthiness, keratin, finite element methods, ansys explicit dynamics, vehicle frame.

1. Introduction

It is quite important to protect the car occupants from dangerous accidents implementing safety systems that avoid vehicle collisions like anti-braking and seat belt systems and etc. A. Alnaqi and S. Yigit worked on a study to find ways for thoracic injuries reduction that are caused by seat belt restraint system in a frontal crash [1]. The other form of occupant protection is crashworthiness which refers to the ability of a vehicle's structure to protect its occupants during an impact. In the design of vehicle structures for impact considerations, it is crucial to carefully control the path of load transformation and optimize both the energy-absorbing process and acceleration pulse. In the event of deformation, the designer should aim to minimize damage to occupants by redirecting the deformation towards energy-absorbing devices, such as the bumper, crash box, and longitudinal side beams. This design approach helps prevent structural parts from intruding into the passenger cabin. Furthermore, controlling the deceleration pulses of the car is essential to reducing the risk of injury during impact, which means maintaining relatively low stiffness. Figure 1 illustrates the load paths in the frontal structure of a vehicle under impact. The blue path (load path 1) signifies the transmission of load through accessories to the bumper, crash box, and longitudinal side beams. Meanwhile, the red path (load path 2) operates through upper rails to the

A-pillar, and the black path (load path 3) involves sub-frames and sill beams.[2]

There are two stages that result from an impact which are compression phase and restitution phase, accompanied with conservation of initial kinetic energy into two forms of energy; firstly dissipation energy in the form of heat, plastic deformation and vibration. The second form of energy is restitution energy in the form of kinetic energy after impact. Hence the absorbed impact energy consists of two parts that are restitution and the important part, which is dissipated energy. The higher the deformation, the higher the dissipated energy is and the lower deceleration pulse. Crashworthiness criteria depend on the nature of the crash. The study of waves in solids aids in estimating the magnitude of stress created by impact or collision of bodies. Hence, a sound knowledge of stress wave propagation in solids is important for a clear understanding of the impact phenomena and some types of fractures A stress wave is transmitted through a body when different parts are not in equilibrium as the case when one solid impinges another. [3]

A. E. Ikpe at [4] worked on design optimization of B-pillar for vehicle crashworthiness in the side impact using FEM Hyper Mesh and CATIA V5 software the comparison was made between two models of the B-pillar. The original model was heavier in mass and made of CP Steel 800/1000, while the optimized one is a reinforcement made of high alloy steel. It is noticed that the von-Mises stress and deformation are lower for optimized model at

* Corresponding author e-mail: awsnammoura@gmail.com.

the same impact force, which is better to protect the passenger from severe damage at the side impact. The situation is different in frontal impact since more energy dissipation needed. Nayan Pundhir [5] did a comparative study between two materials when the simplified model of vehicle body moves at constant velocity of 15m/s and collides with a pole composed of structural steel at different impact positions. The vehicle body is made of one of two materials which are High density polyethylene/multi walled carbon nanotube-polymer composite (HDPE/MWCNT) and High-density polyethylene/kenaf fiber reinforced polymer composite (HDPE/kenaf). The research conduct on that HDPE/kenaf has higher crashworthiness than HDPE/MWCNT model and exposed to higher von misses stress. H. D. Gopalakrishna et al [6] they did a crashworthiness analysis of vehicle body panel collides with a rigid pole and comparing five different materials the body panel is made of that are structural steel NL, Aluminum NL, Steel v250, Aluminum 6061-T6, polycarbonate and the results show that the polycarbonate has higher specific energy absorption. Shu-Tian ,Tong ,Tang and Zhang [7] They did a research topic and simulation about crashworthiness of S-shaped front rails made of mild steel by changing the cross section of the rail three groups of cross sections were investigated which are regular polygonal, non-convex polygonal and multi cell sections with inner member and energy absorption comparison were made. Mingming Wu and Xueping Zhang [8] worked on safety improvement when side impact behavior involved by adding reinforcements without compromising the functionality of existing components.

Balcha ,Bhaskaran J etc [9] worked on increase compression strength of vehicle bumper using Banana fiber reinforced polymer composite. This paper shows the work on the use of bio-inspired keratin material in the vehicle bumper during frontal offset impact. Keratin is a structural protein that exists in the outer coverings of the

vertebrates. It is a ubiquitous biological polymer comprising the bulk of mammalian, avian, and reptilian epidermal appendages, including nails, hair, the outer layer of skin, feathers, beaks, horns, hooves, whale baleen, claws, scales, hagfish slime, and gecko pads [10-12]. Keratinized materials has wide features and characteristics include toughness which means high energy absorption and impact resistance as found in animal horns and hooves. Additionally it also light in weight and stiff which provides buckling resistance as found in feathers due to aerodynamic load. Keratin material is a multifunctional biological material that can be utilized as a raw material in fiber-reinforcement composites. Keratin is produced by cells called keratinocytes; those cells will die after the production hence keratin is unlike bones nor collagen as the cells of others nutrition to maintain its characteristics [13]. Mechanical properties such as Young's modulus, yield strength, and impact resistance are predominant features related to horns of animals considered futuristic for biological safety and impacts resistance structures in crashworthiness tests for automotive and aerospace applications.[14].

2. Methodology

Experimental crash tests involve the destruction of several vehicles and are time-consuming, making them an uneconomical process. Therefore, the most cost-effective initial choice is to use Finite Element Analysis (FEA), which solves complicated problems based on partial differential equations and mathematics [15]. Various types of software are available for crash test simulations, including LS-Dyna, ABAQUS, RADIOSS, and others [16]. In this paper, ANSYS Explicit Dynamics was chosen as the software to conduct the simulation. The model used is a 3D CAD model of an Audi R8 spaceframe obtained from the GrabCAD website. Figure 2 shows the prepared model and its dimensions for the bounding box.

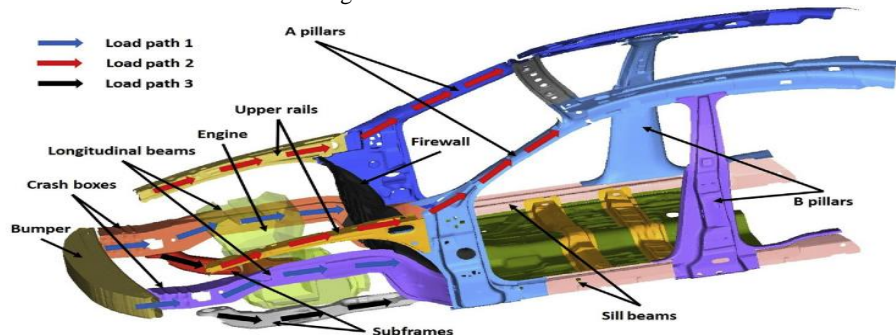


Figure 1. Load paths of the vehicle frontal structure at the event of frontal impact.

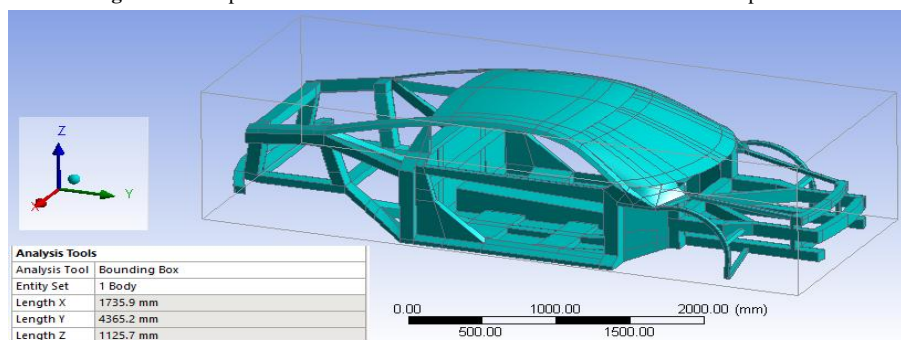


Figure 2. Audi R8 spaceframe 3D CAD model and import the model in ANSYS software

The next step is make a mirror of the vehicle model to generate another one, then translate it in the x-axis direction by 0.5 m to perform frontal offset impact then apply the chosen material to the vehicle bumper. The materials of the bumper are structural steel NL taken from the engineering data library of Ansys program and keratin horn sheep material data obtained from M. Mysore, Y. Patil, et [17] that extract the mechanical and physical properties from different test coupons of keratin horn sheep material where the results shows that this material is anisotropic material that has different mechanical properties with different orientations. Many attempts has been done for anisotropic property representation in the model using Ansys composite Prepost (ACP) and material designer and MCalibration without successful arrive due to missed data about this material. Therefore, the last choice that was taken is isotropic assumption for longitudinal orientation of keratin horn sheep material and Poisson's ratio of 0.4 based on research papers [18-19]. Table 1 shows the properties of structural steel NL, keratin horn sheep material.

The selected mesh for both vehicles of 40 mm body sizing and the other runs with 10mm size in frontal region of the model. The simulation analysis settings specify an end time of 35 ms. For the initial conditions, a comparison between steel and keratin bumper models was conducted over a wide range of relative collision speeds, ranging from 20 to 100 m/s. Measurements were taken at various paths and specific vertex points throughout the vehicle structure, with variable material assignments for the bumper, as illustrated in Figure 3. It is important to know that the total length of frontal path is 1799mm and 1848.9mm for each left and right paths.

2.1. Assumptions

Before describing and showcasing the simulation results, it is important to consider several assumptions for model simulation, which are as follows:

1. both vehicle's structure is constructed from structural steel NL. However, one of the vehicles bumper is made of structural steel, and the other is made of horn sheep keratin, both with a thickness of 3mm. It is assumed that the keratin exhibits isotropic properties.
2. Road loads like rolling resistance, friction and aerodynamic resistance is negligible.
3. Neglect the existence of tires, accessories, engine, and other vehicle components. This neglect leads to the disregard of load and weight distribution in the model and the vehicle chassis.

Since the two vehicles are the same, the front of each one is at the same level as the other, so that the height of the bumper of the first vehicle is the same as the height of the bumper of the second vehicle

Table 1. Mechanical and physical properties for each material applied in the vehicle bumper.

| Material property | Structural steel NL | Keratin horn sheep |
|------------------------------|---------------------|--------------------|
| Density [kg/m ³] | 7850 | 1231 |
| Young's modulus [MPa] | 200000 | 6500 |
| Poisson's ratio | 0.3 | 0.4 |
| Yield strength [MPa] | 250 | |
| Bulk modulus [MPa] | 166670 | 10833 |
| Shear modulus [MPa] | 76923 | 2321.4 |
| Tangent modulus [MPa] | 1450 | --- |
| Specific heat [J/kg.C] | 434 | 1530 |

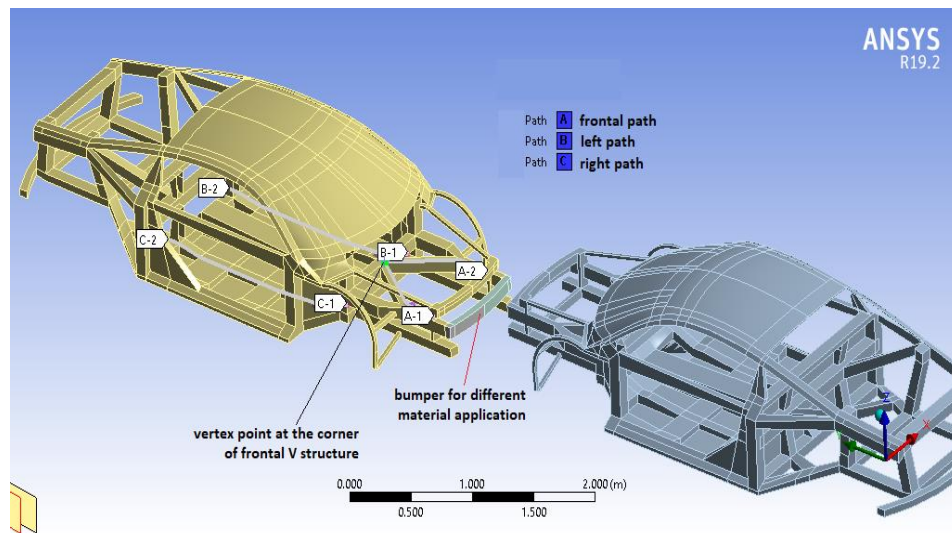


Figure 3. Different paths for measurement of simulation results.

3. Results and discussion

3.1. Equivalent stress at wide range of collision speeds

Equivalent von-Mises stress and equivalent plastic strain were measured through the selected measurement regions in Fig. 3 at the chosen vertex point. The comparison of equivalent von-Mises stress between steel and keratin bumper models is shown in Fig. 4 over a wide range of relative collision speeds, ranging from 20 to 100 m/s. It can be noticed that the keratin bumper model is subjected to higher von-Mises stress, indicating a higher tendency to yield, with greater plastic deformation. This denotes higher impact energy dissipation, reducing the danger of deceleration pulses compared with the steel bumper model. However, one measurement point is not sufficient, so the observation should be extended along paths for a more accurate assessment as discussed later.

Fig. 5 shows the stress contours through the structures of the colliding vehicles as a result for an offset frontal impact simulation at a specified relative speed. The fracture of the rear sub-frame can be seen in the right vehicle in the picture. This denotes the importance of taking path measurements even through the bottom of the occupant region in vehicles, such as the left and right paths.

3.2. Frontal path analysis

Fig. 6 illustrates the simulation results for (a) the steel bumper model and (b) the keratin bumper model at a relative impact speed of 100 m/s along the frontal path, with a mesh element size of 10 mm. This path has a total length of 1799.7 mm, while the other collided car is hidden from view. It is observed that the von Mises stress—and consequently, the strain values are higher in the keratin

bumper model. For example, near the end of the path, the stress peak difference is 156 MPa, indicating the dominance of stress in the keratin bumper model. From the left side of the figure, which depicts the limited bumper system, it is evident that the keratin model exhibits significantly greater twisting and bending in its deformation path compared to the steel model. This suggests that the keratin material may be inherently more flexible or prone to localized deformation under load, which could potentially enhance its energy absorption characteristics.

In contrast, the steel model's deformation path is relatively more uniform and less twisted. These differences are critical for evaluating crashworthiness: while the increased deformation in the keratin model might allow it to dissipate energy more effectively by accommodating higher strains, the steel model's controlled deformation could help maintain structural integrity during an impact.

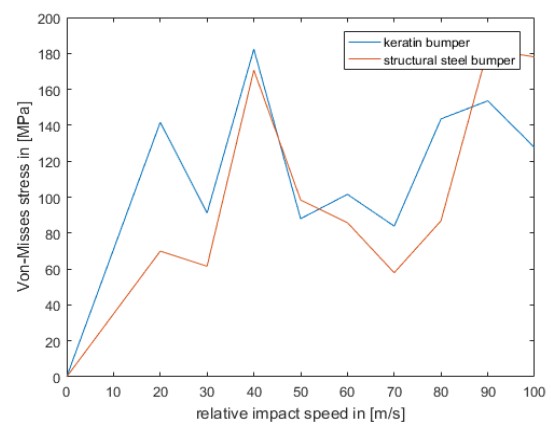


Figure 4. Equivalent von-Mises stress versus relative speeds comparison between keratin and steel bumper models during 35ms of end time

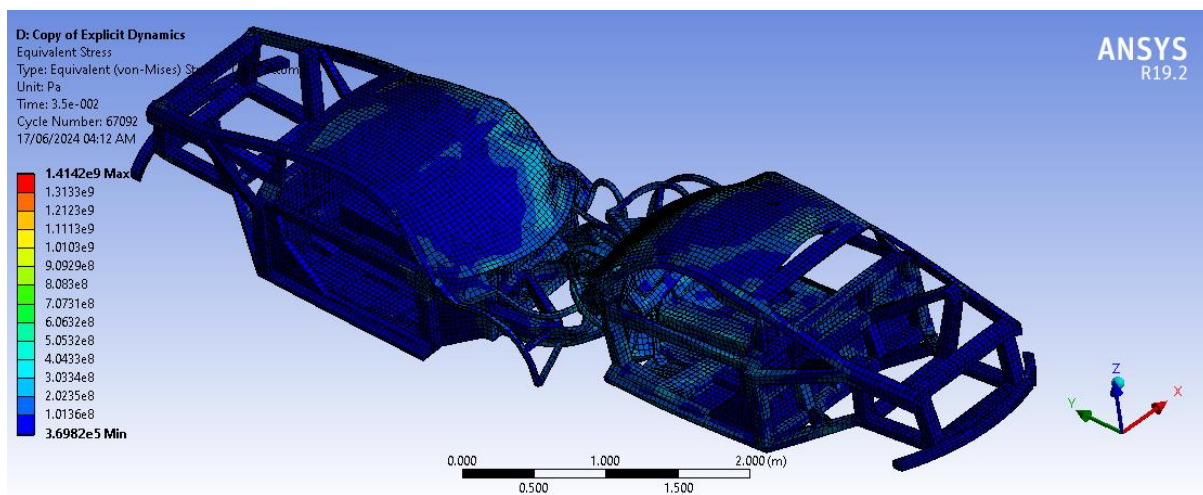


Figure 5. Von-Mises stress contours through vehicles spaceframe as a result of half frontal impact at relative impact speed of 60m/s.

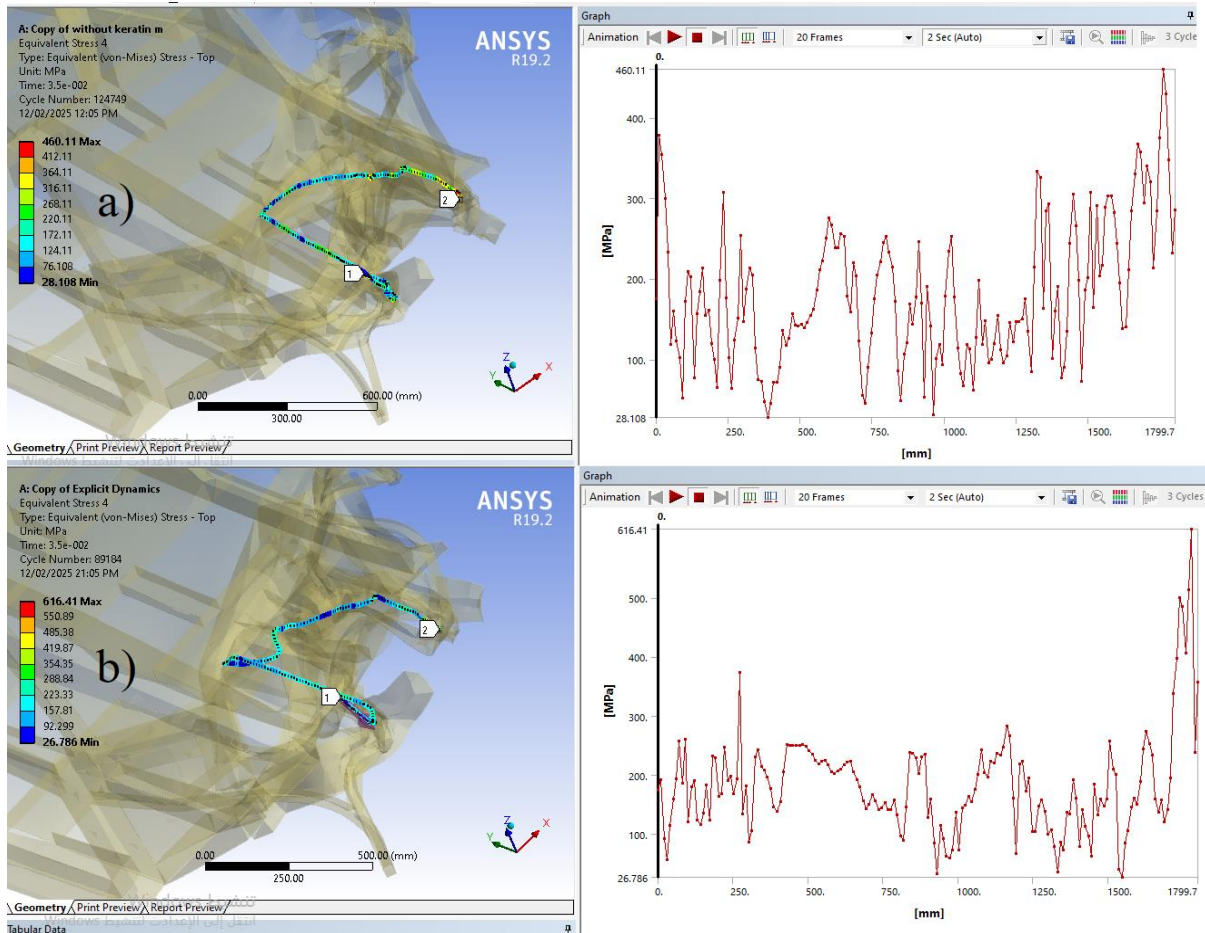


Figure 6. Stress contours through the frontal path when the relative collision speed is 100m/s
 a) steel bumper model b) keratin horns sheep bumper model

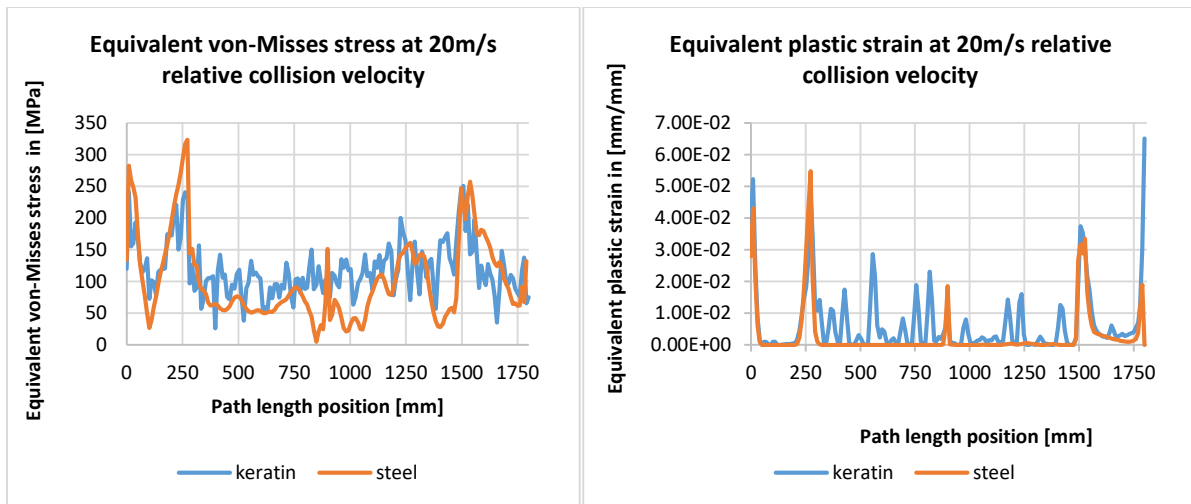


Figure 7. Equivalent von-Mises stress and Equivalent plastic strain versus path length position through the frontal path region at 20m/s of relative collision velocity.

Fig. 7 shows the equivalent von Mises stress and plastic strain curves along the frontal path for a relative collision velocity of 20 m/s. It is observed that the steel bumper model exhibits higher stress peaks than the keratin model, particularly around the beginning of the path (0 mm), 250 mm, and 1567 mm. In contrast, the rest of the path shows higher stress values for the keratin model. Additionally,

the stress distribution in keratin is more uniform and less pronounced in terms of peak variations compared to steel. This results in smoother and lower stress fluctuations, allowing for gradual load transmission without excessive stress accumulation in specific locations, as seen in steel. The higher stress peaks in the steel model indicate greater localized failure risks, especially when the stress

significantly exceeds the yield strength of structural steel, which is 250 MPa.

Also, when looking at the plastic strain curve, which represents permanent deformation, it is observed that the keratin bumper model exhibits more plastic deformation in the frontal path compared to steel. This indicates higher energy dissipation.

Fig. 8 shows the von Mises stress and plastic strain versus path length results at an 80 m/s relative impact speed. The keratin model generally exhibits higher stress distribution compared to the steel model along most of the path length, except around the 1300 mm position. In general, greater plastic strain is observed at this velocity compared to the 20 m/s speed discussed previously in Fig. 7. This is due to the higher equivalent stress values exceeding the yield strength of structural steel NL. For

instance, at the 0 mm position, the stress is 288 MPa for steel and 378 MPa for keratin, with both values exceeding 250 MPa, which is the yield strength of structural steel NL.

Within the 375 mm to 735 mm position range at 80 m/s, no plastic strain is observed because the von Mises stress remains below 250 MPa. However, higher plastic strain peaks and greater deformation are seen in the steel bumper model at the end of the path compared to keratin. In contrast, within the first 211 mm of the path length, the keratin bumper model shows higher deformation, but it is lower in the second half. Generally as noted in the curve the greater deformation in the steel model at high speed suggests that it is more effective in energy dissipation at higher collision speeds than keratin. This is because material properties vary with strain rate, and the strain rate increases with collision speed.

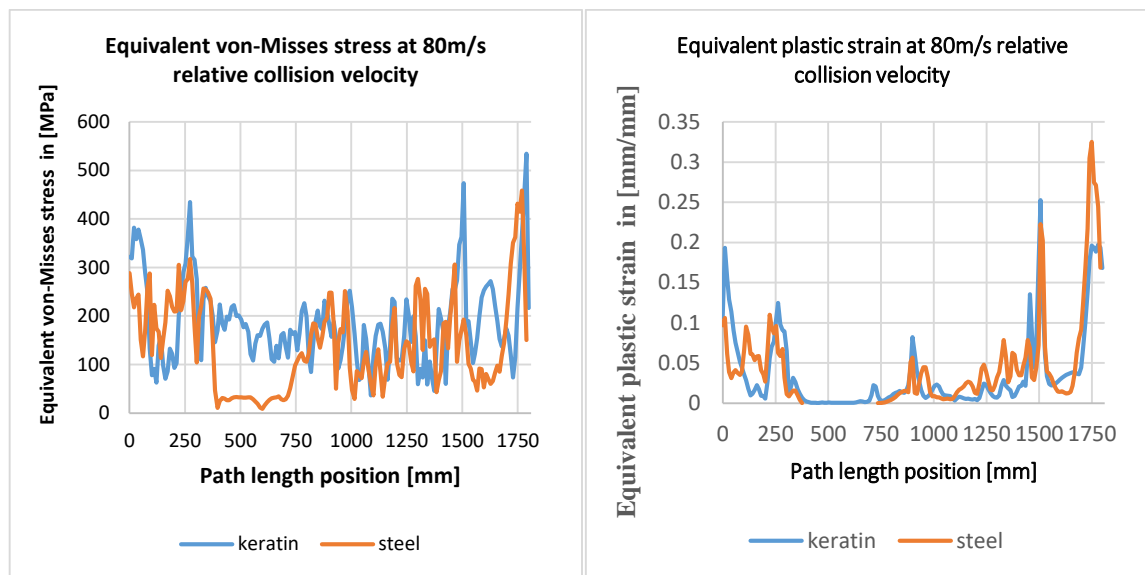


Figure 8. Equivalent von-Mises stress and Equivalent plastic strain versus path length position through the frontal path region at 80m/s of relative collision velocity.

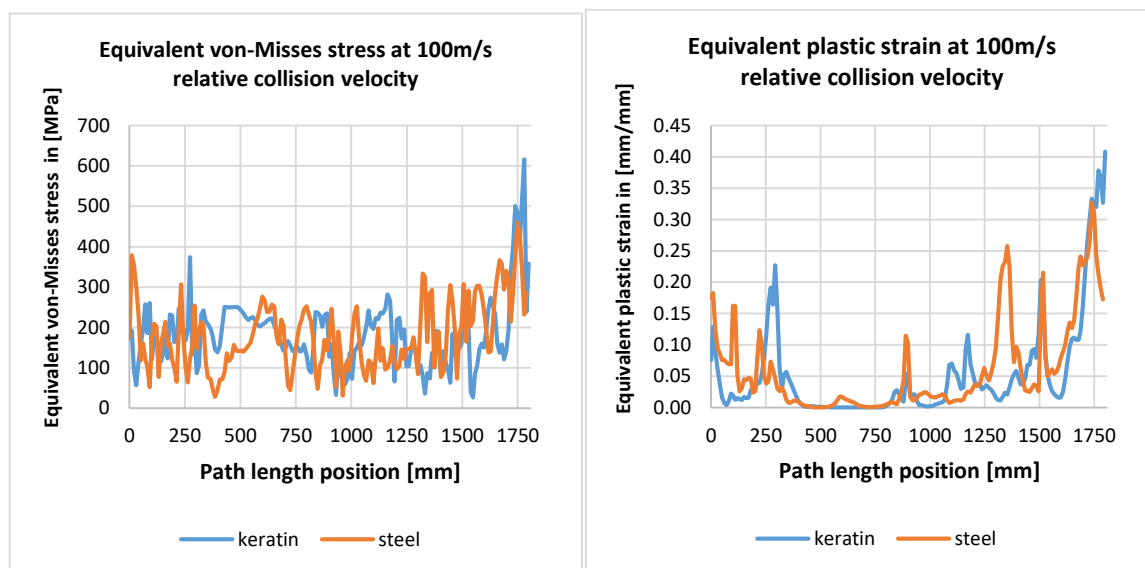


Figure 9. Equivalent von-Mises stress and Equivalent plastic strain versus path length position through the frontal path region at 100m/s of relative collision velocity

in Figure 9, where the relative impact speed is 100 m/s, higher stress peaks and consequently higher plastic strain are observed in the keratin model around the regions of 272mm, 1066mm, and 1739 mm along the path. The steel bumper shows significant dominance over the keratin model in terms of plastic strain around the 110 mm and 1342 mm positions. Some locations exhibit considerable plastic strain even when the von-Mises stress is less than the yield strength of structural steel NL. For example, at a position of 1517.2 mm, as shown, the steel model has a plastic strain of 0.21532 mm/mm despite a stress of 164.36 MPa. In comparison, the keratin model has a plastic strain of 0.17855 mm/mm with a stress of 210.19 MPa. This will be explained in Fig. 10.

Fig. 10 shows the stress curves over time at a point located at a length position of 1517.2 mm in the frontal path. The graph reveals the transient response nature of the von-Mises stress and its fluctuations over time. Yielding begins at 7 ms in the keratin model, reaching a peak of 286.8 MPa at 28 ms, while yielding in the steel model begins at 14 ms, with a peak of 400.63 MPa at 21 ms. A significantly higher stress curve is observed for the steel model compared to keratin between 14 and 28 milliseconds, resulting in higher plastic strain. By the end

time of 35 ms, the von-Mises stress drops below the yield strength, which explains the presence of plastic strain despite the lower stress levels yield at the end time.

3.3. Left path analysis

Fig.11 shows the von-Mises stress and equivalent plastic strain curves along the left path length, with measurements taken through the left side of the vehicle structure where the occupants are located, 35 ms after the collision. The distribution of von-Mises stress along this path is due to stress wave propagation, which transmits stress waves to locations far from the source of impact. This explains the rear subframe fracture observed in Fig. 5. Additionally, it is noted that the equivalent plastic strain is zero when the relative collision speed is 20 m/s, after 65 mm along the path length axis, as shown in the right of Fig. 11. This occurs because the equivalent von-Mises stress on the path length axis is less than 200 MPa, which is significantly below the yield strength of the structural steel NL material of the vehicle structure, meaning the stress does not reach the yield value during the 35 ms of simulation time.

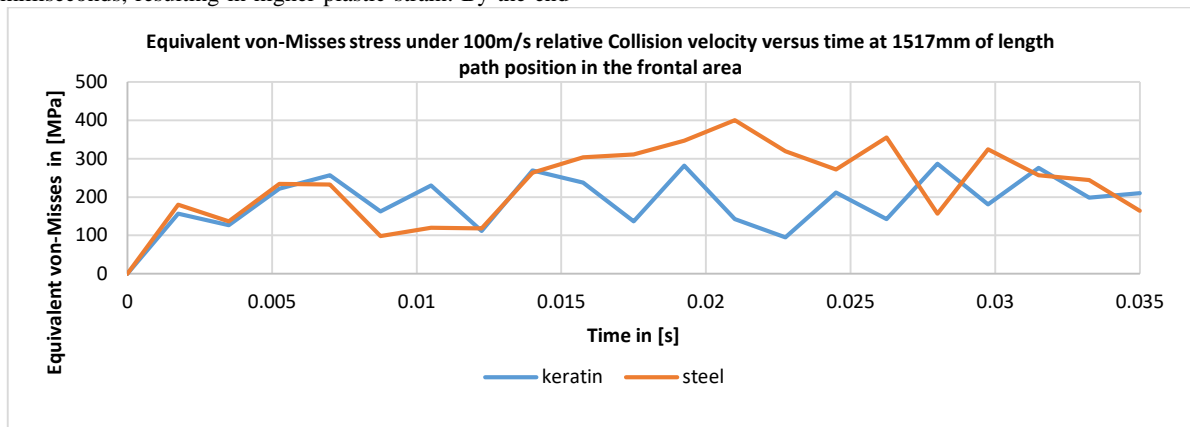


Figure 10. Equivalent von-Mises stress with time at vortex point locate at the angle between the left rail and inclined beam in 1517.2mm of position length in the frontal region.

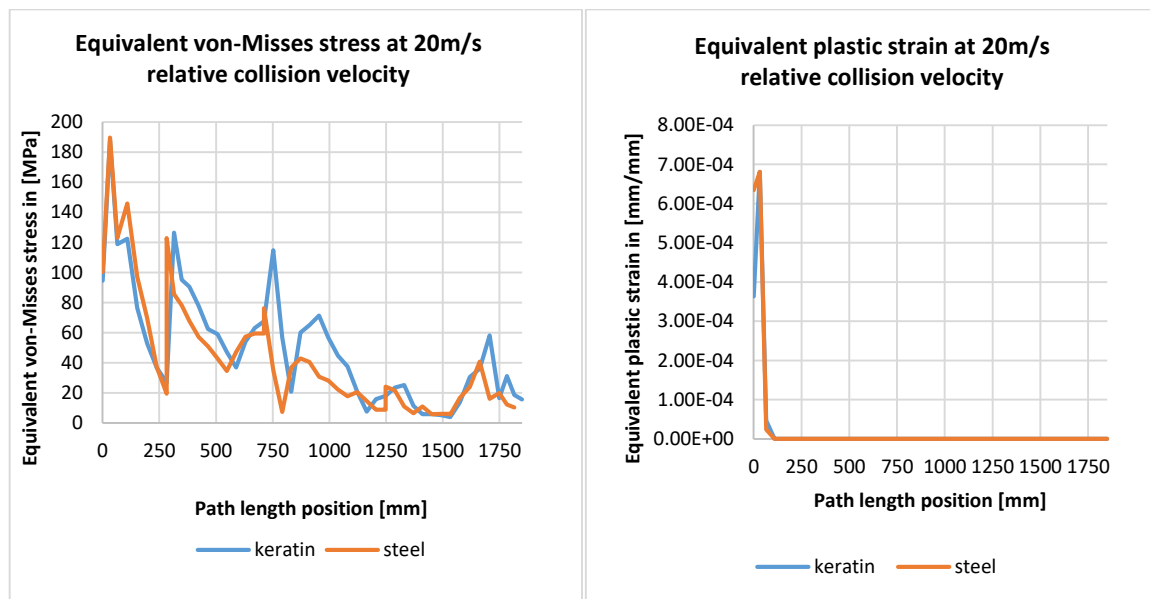


Figure 11. Equivalent von-Mises stress and Equivalent plastic strain versus path length position through the left path region at 20m/s of relative collision velocity.

Fig. 12 shows the results at relative speed of 80 m/s, higher stress peaks in keratin model and higher stress curves observed than the steel model along the first 282 mm of path length and between 711 mm and 833 mm. However, the plastic strain curves are almost identical, with negligible differences. This is due to the transient response of stress in impact mechanics. The stress in the steel model changes over the 35 ms interval, resulting in strain nearly coincident with the keratin strain curve, as previously discussed in Fig. 10.

Fig. 13 at a relative collision speed of 100 m/s, the peaks of the stress curves for keratin and steel reach 545.6 MPa and 327.3 MPa at 32 mm and 282.4 mm along the length path position, respectively. In general, the keratin model exhibits higher plastic strain, with a peak of 0.2 mm/mm, compared to the steel model's peak

of 0.14516 mm/mm, with the only region where the plastic strain of the steel model is higher being around 282.4 mm.

3.4. Right path analysis

Fig. 14 illustrates the Equivalent von-Misses stress and plastic strain curves versus path length at relative impact velocity of 20m/s, the measurements taken along the right path inside the bottom of vehicle structure. It is clear that lower stress and strain are localized along the right path compared to the left path, as the latter is closer to the point of impact and disturbance. Zero plastic strain observed along the entire path except the first 65mm in keratin model. And zero plastic strain exhibited due to very much stress below the yield strength.

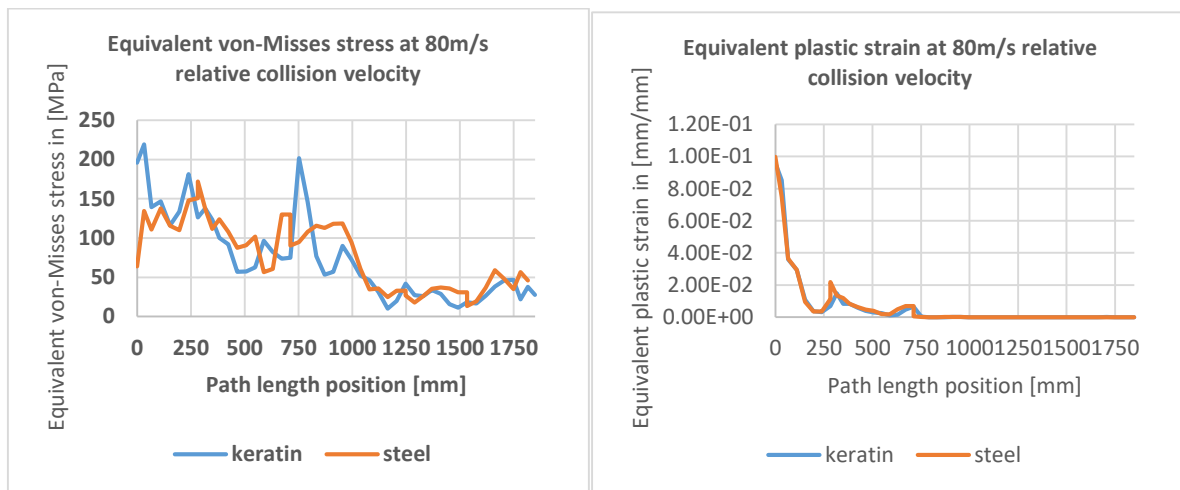


Figure 12. Equivalent von-Misses stress and Equivalent plastic strain versus path length position through the left path region at 80m/s of relative collision velocity.

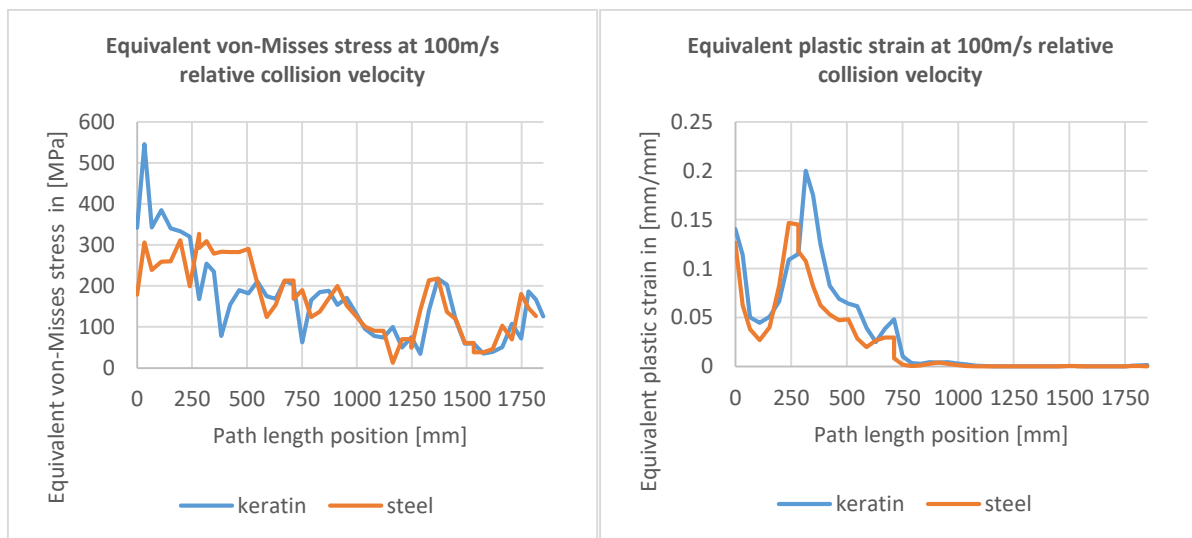


Figure 13. Equivalent von-Misses stress and Equivalent plastic strain versus path length position through the left path region at 100m/s of relative collision velocity.

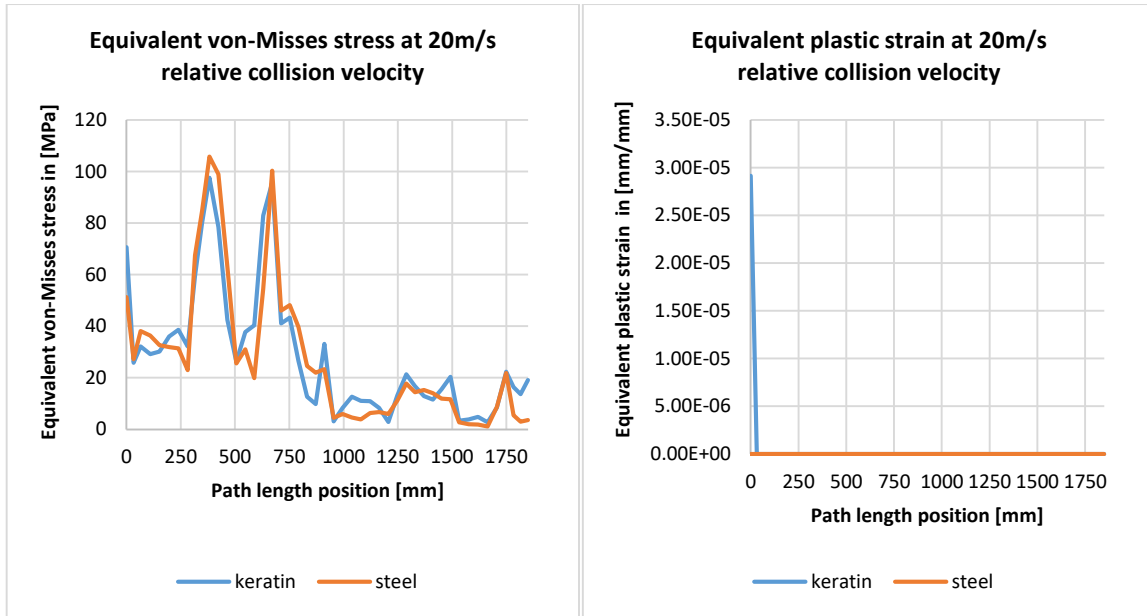


Figure 14. Equivalent von-Mises stress and Equivalent plastic strain versus path length position through the right path region at 20m/s of relative collision velocity.

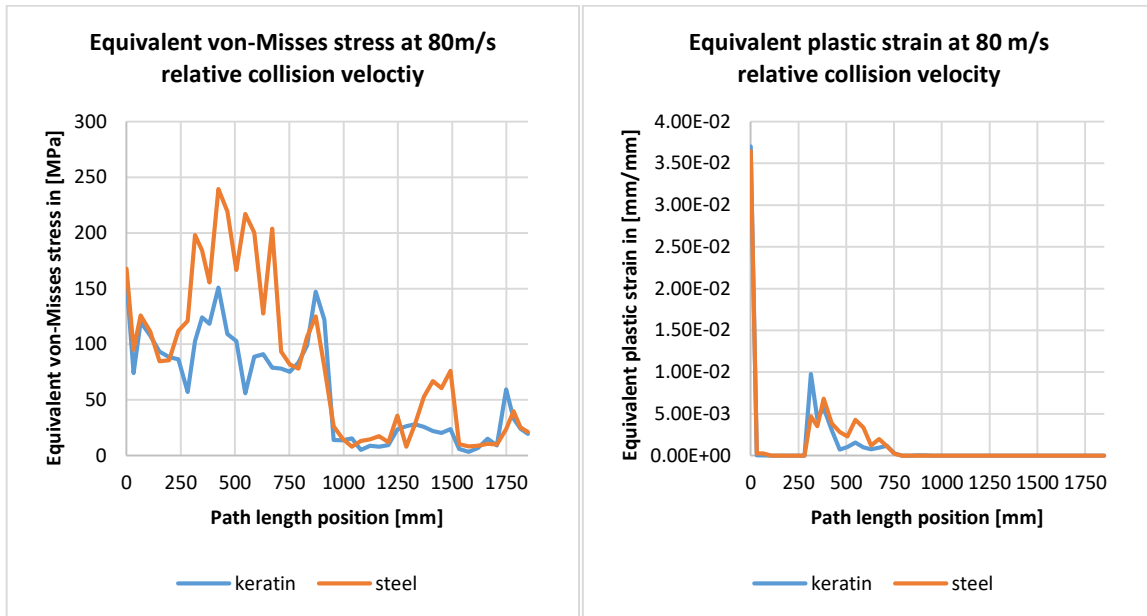


Figure 15. Equivalent von-Mises stress and Equivalent plastic strain versus path length position through the right path region at 80m/s of relative collision velocity.

Fig. 15 shows the results at 80 m/s of relative collision velocity, the von-Mises stress peaks and curves is greater for steel model compared with keratin model except the first 196mm of path length where the curves are coincident and a round 871mm of path length position where the keratin model stress is little higher by 40 MPa. Non-zero plastic strain is observed only at 0 mm and from 285 mm to 711 mm along the path length.

Fig. 16 shows the results at 100m/s of relative collision velocity it's noted that higher Equivalent von-Mises stress for steel model at the first 589 mm of path length position and higher plastic strain at the same region means more permanent deformation and energy dissipation and the rest of path region consist of higher stress in keratin but there is no plastic strain.

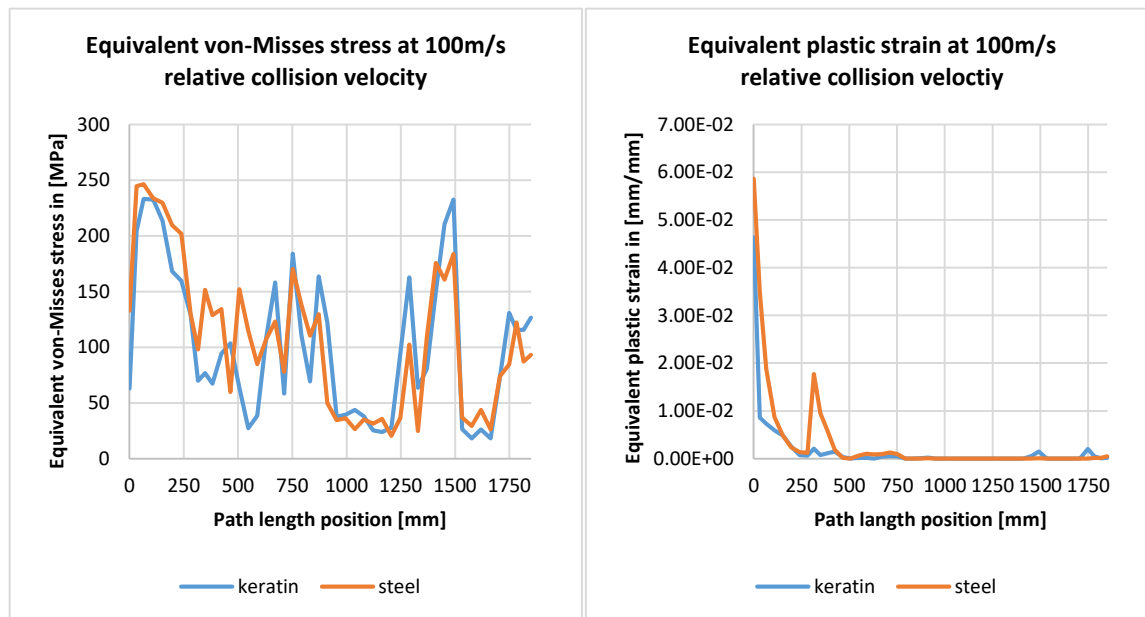


Figure 16. Equivalent von-Mises stress and Equivalent plastic strain versus path length position through the right path region at 100m/s of relative collision velocity.

4. Conclusion

A simulation of a vehicle-to-vehicle frontal offset impact was conducted using **ANSYS Explicit Dynamics** to improve crashworthiness and energy dissipation. The **bio-inspired keratin (sheep horn) bumper material** demonstrated excellent energy dissipation at low impact speeds. The results showed that **higher von Mises stress and greater plastic deformation** occurred throughout the vehicle structure at low impact speeds when the bumper material was keratin. **This higher plastic deformation led to greater energy dissipation**, which helped **reduce forces and deceleration pulses transmitted to occupants**, thereby minimizing the risk of serious injuries. Consequently, the **keratin bumper model suggests better crashworthiness behavior** compared to the **steel bumper model at low speeds**. However, at **high impact speeds**, the **steel bumper model performed better** due to **brittle behavior of keratin and the strain rate sensitivity effect of steel**, which increases its strength under high deformation rates. Additionally, since **keratin has a lower strength than steel**, it deforms **earlier and more easily** at low speeds.

References

- [1] A.A. Alnaqi and A.S. Yigit, "Dynamic Analysis and Control of Automotive Occupant Restraint Systems", *Jordan Journal of Mechanical and Industrial Engineering*, Vol.5, no.1,(2011),pp. 39 – 46
- [2] Dario Vangi, *Vehicle Collision Dynamics Analysis and Reconstruction*, Butterworth-Heinemann; 1st edition , January 20, 2020.
- [3] Fraige, F. Y., & Es-Saheb, M. H. (2022). Analysis of elastic stress wave propagation in stepped bars, transmission, reflection, and interaction: Experimental investigation. *Jordan Journal of Mechanical and Industrial Engineering*, 16(2), 261–274.
- [4] Ikpe, A. E., Owunna, I. B., & Satope, P. (2017). Design optimization of a B-pillar for crashworthiness of vehicle side impact. *JOURNAL OF MECHANICAL ENGINEERING AND SCIENCES*, 11(2), 2693–2710. doi.org/10.15282/jmes.11.2.2017.11.0245
- [5] Nayan Pundhir, Himanshu Pathak and Sunny Zafar, "Crashworthiness of automobile made of HDPE/kenaf and HDPE/MWCNT polymer composites", IOP Conf. Series: Journal of Physics: Conf. Series 1240 (2019) 012098.
- [6] Gopalakrishna, H., Panda, P.K., Jois, P.K., & Nihilp, N. (2014). CRASHWORTHINESS OF AUTOMOBILE IN A VEHICLE-TO-POLE CRASH SIMULATION
- [7] Liu, ST., Tong, ZQ., Tang, ZL. et al. Design optimization of the S-frame to improve crashworthiness. *Acta Mech Sin* 30, 589–599 (2014)
- [8] Wu, M., & Zhang, X. (2022). Optimal control method for side impact safety of vehicle frame structure. *Jordan Journal of Mechanical and Industrial Engineering*, 16(1), 41–51.
- [9] R. Balcha, J. Bhaskaran, P. J. Ramulu, and B. B. Tesfamariam, "Mechanical behaviour assessment of banana fibres reinforced polymeric composite with aluminium-powder filler," *Jordan Journal of Mechanical and Industrial Engineering*, vol. 17, no. 2, pp. 269–279, Jun. 2023. doi: 10.59038/jjmie/170210.
- [10] Fraser, R.D.B., MacRae, T.P., and Rogers, G.E.(1972). Keratins: their composition. *Struct.Biosynthesis* 52, 29–30.
- [11] McKittrick, J., Chen, P.Y., Bodde, S.G., Yang, W., Novitskaya, E.E., and Meyers, M.A. (2012). The structure, functions, and mechanical properties of keratin. *Jom* 64, 449–468
- [12] Meyers, M.A., Chen, P.Y., Lin, A.Y.M., and Seki, Y.(2008). Biological materials: structure and mechanical properties. *Prog. Mater. Sci.* 53, 1–206.
- [13] McKittrick, J., Chen, P.Y., Bodde, S.G. et al. The Structure, Functions, and Mechanical Properties of Keratin. *JOM* 64, 449–468 (2012)
- [14] Tombolato, L.; Novitskaya, E.E.; Chen, P.Y.; Sheppard, F.A.; McKittrick, J. Microstructure, elastic properties and deformation mechanisms of horn keratin. *Acta Biomater.* 2010, 6, 319–330.

- [15] A. Muhammad, and I. H. Shanono, "Static Analysis and Optimization of a Connecting Rod," International Journal of Engineering Technology and Sciences, vol. 6, no. 1, pp. 24-40, 2019.
- [16] Yadav, S.; Pradhan, S. Investigations into Dynamic Response of Automobile Components during CrashSimulation. *Procedia Eng.* 2014, 97, 1254–1264
- [17] Mysore THM, Patil AY, Raju GU, Banapurmath NR, Bhovi PM, Afzal A, Alamri S, Saleel CA. Investigation of Mechanical and Physical Properties of Big Sheep Horn as an Alternative Biomaterial for Structural Applications. *Materials.* 2021; 14(14):4039. <https://doi.org/10.3390/ma14144039>
- [18] Kitchener, A., Vincent, J.F.V. Composite theory and the effect of water on the stiffness of horn keratin. *J Mater Sci* 22, 1385–1389 (1987). <https://doi.org/10.1007/BF01233138>
- [19] Drol, C. J., Kennedy, E. B., Hsiung, B. K., Swift, N. B., & Tan, K. T. (2019). Bioinspirational understanding of flexural performance in hedgehog spines. *Acta biomaterialia*, 94, 553-564.